ACCOUNTS of chemical research

Article

pubs.acs.org/accounts

Adsorption and Reactions of O_2 on Anatase TiO_2

Ye-Fei Li,[†] Ulrich Aschauer,[‡] Jia Chen,[†] and Annabella Selloni*,[†]

[†]Department of Chemistry, Princeton University, Princeton, New Jersey 08544, United States

[‡]Materials Theory, ETH Zurich, 8093 Zürich, Switzerland

CONSPECTUS: The interaction of molecular oxygen with titanium dioxide (TiO_2) surfaces plays a key role in many technologically important processes such as catalytic oxidation reactions, chemical sensing, and photocatalysis. While O_2 interacts weakly with fully oxidized TiO_2, excess electrons are often present in TiO_2 samples. These excess electrons originate from intrinsic reducing defects (oxygen vacancies and titanium interstitials), doping, or photoexcitation and form polaronic Ti^{3+} states in the band gap near the bottom of the conduction band. Oxygen adsorption involves the transfer of one or more of these excess electrons to an O_2 molecule at the TiO_2 surface. This results in an adsorbed superoxo (O_2^-) or peroxo (O_2^{2-}) species or in molecular dissociation and formation of two oxygen adatoms ($2 \times O^{2-}$). Oxygen adsorption is also the first step toward oxygen incorporation, a fundamental reaction that strongly affects the chemical properties and charge-carrier densities; for instance, it can transform the material from an n-type semiconductor to a poor electronic conductor.

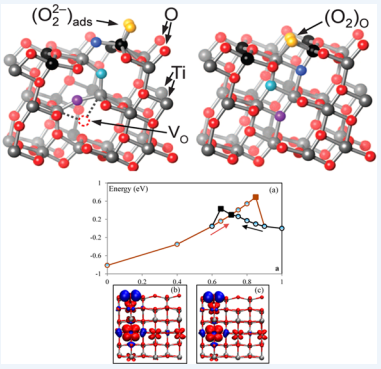

In this Account, we present an overview of recent theoretical work on O_2 adsorption and reactions on the reduced anatase (101) surface. Anatase is the TiO_2 polymorph that is generally considered most active in photocatalysis. Experiments on anatase powders have shown that the properties of photoexcited electrons are similar to those of excess electrons from reducing defects, and therefore, oxygen on reduced anatase is also a model system for studying the role of O_2 in photocatalysis. Experimentally, the characteristic Ti^{3+} defect states disappear after adsorption of molecular oxygen, which indicates that the excess electrons are indeed trapped by O_2. Moreover, superoxide surface species associated with two different cation surface sites, possibly a regular cation site and a cation close to an anion vacancy, were identified by electron paramagnetic resonance spectroscopy. On the theoretical side, however, density functional theory studies have consistently found that it is energetically more favorable for O_2 to adsorb in the peroxo form rather than the superoxo form. As a result, obtaining a detailed understanding of the nature of the observed superoxide species has proven difficult for many years.

On reduced anatase (101), both oxygen vacancies and Ti interstitials have been shown to reside exclusively in the susbsurface. We discuss how reaction of O_2 with a subsurface O vacancy heals the vacancy while leading to the formation of a surface bridging dimer defect. Similarly, the interaction of O_2 with a Ti interstitial causes migration of this defect to the surface and the formation of a surface TiO_2 cluster. Finally, we analyze the peroxo and superoxo states of the adsorbed molecule. On the basis of periodic hybrid functional calculations of interfacial electron transfer between reduced anatase and O_2, we show that the peroxide form, while energetically more stable, is kinetically less favorable than the superoxide form. The existence of a kinetic barrier between the superoxo and peroxo states is essential for explaining a variety of experimental observations.

INTRODUCTION

Titanium dioxide is one of the most widely used photocatalytic materials because of its abundance and high stability in different environments and conditions.[1−4] TiO_2 has several polymorphs, rutile and anatase being the most common. While rutile is the thermodynamically most stable bulk phase, anatase is stable in nanoparticles[5] and shows a higher photocatalytic activity,[6] making it the most interesting phase for use in high-surface-area photocatalytic and photovoltaic devices.[7] Molecular oxygen plays a key role in many TiO_2-based photocatalytic processes; in particular, O_2 adsorbed on TiO_2 surfaces is known to act as an electron scavenger and is often used to suppress electron−hole recombination, which increases the lifetime of the excited state and thus the yield of the photocatalytic reaction.[1,8] The interaction of TiO_2 with O_2 molecules has therefore attracted considerable interest for decades.

Electron transfer from the surface to the oxygen molecule is essential for oxygen adsorption. In fact, O_2 does not adsorb on stoichiometric TiO_2; excess electrons are required. As titania samples are very often reduced,[2] excess electrons originating from oxygen vacancies and titanium interstitials are typically present in the material. These excess electrons form Ti^{3+} states in the band gap near the bottom of the conduction band[2,9] and are responsible for the n-type conductivity that is important in many applications of TiO_2, from photocatalysis to water splitting and dye-sensitized solar cells. Besides controlling the conductivity, oxygen vacancies and Ti interstitials also play a central role in the surface chemistry of TiO_2.[1−4] Both defects

Special Issue: DFT Elucidation of Materials Properties

Received: December 23, 2013
Published: April 17, 2014

were recently shown to exist exclusively in the subsurface region in the case of anatase (101),[10−12] the majority surface of this TiO_2 polymorph. This is a significant difference with respect to the widely studied rutile (110) surface, where a large concentration (∼5−10%) of surface oxygen vacancies is typically observed under ultrahigh vacuum conditions.[2]

In comparison with the numerous surface science studies of O_2 on defective rutile TiO_2(110),[2,13−17] atomic-scale information on the interaction of oxygen with reduced anatase surfaces is more limited. Experimentally, there is evidence that various surface species are formed upon O_2 adsorption. In particular, electron paramagnetic resonance (EPR) measurements on anatase powders have identified two long-lived superoxide (O_2^-) species associated with different cation surface sites.[8,18] In Scanning tunneling microscopy (STM) studies on single-crystal anatase (101),[19] surface species resulting from the reactions of O_2 with both regular and defect surface sites have been observed. On the theoretical side, studies based on density functional theory (DFT) have also reported a few different species, notably a superoxide species and a peroxide species, at regular undercoordinated surface Ti sites.[19−21] The peroxide, however, has been consistently found to be more stable than the superoxo form, in apparent contradiction with the EPR experiments.

In this Account, we present an overview of recent theoretical investigations of O_2 on the anatase (101) surface, with the aim of highlighting technical difficulties as well as new physical/chemical insights provided by these studies. After discussing some characteristics of oxygen vacancies and Ti interstitials in reduced TiO_2, we examine the reactions of O_2 with intrinsic subsurface defects at anatase (101) and conclude with a discussion of recent studies that allow us to provide a consistent explanation of experimental observations.

■ INTRINSIC REDUCING DEFECTS IN ANATASE

Titania samples in the form of powders, single crystals, or thin films are very often reduced and electrically conducting. The reduction is associated with a change in the oxidation state of the transition-metal ion from formally Ti^{4+} in stoichiometric TiO_2 to Ti^{3+} in the reduced samples. Calculations based on DFT in the local density approximation (LDA) or semilocal generalized-gradient approximation (GGA)[22] have proven inadequate to describe these Ti^{3+} species.[9,23] Local and semilocal functionals are indeed affected by the self-interaction error,[24] which often results in a spurious delocalization of the electronic states. Two main approaches are generally used to overcome this problem, DFT+U methods[25] and hybrid functionals.[26,27] Although limited by the presence of parameters that are difficult to evaluate fully ab initio (i.e., the value of U in DFT+U or the fraction of exact Hartree−Fock exchange to be added to the DFT exchange in hybrid methods), these approaches usually provide results that are more accurate than those of standard DFT for the electronic properties (band gaps, defect energy levels, etc.) of semiconducting and insulating materials.

Oxygen Vacancy (V_O)

The removal of one neutral lattice oxygen atom leaves two extra electrons (assuming a formal −2 oxidation state of O in TiO_2). Differently from ionic solids, where the extra electrons are localized in the cavity formed by the missing anion and are stabilized by the strong Madelung potential, in TiO_2 the two electrons prefer to fill empty states of Ti ions, resulting in Ti^{3+} species. These two electrons may pair up to give a closed-shell singlet state or form open-shell singlet or triplet states.

At the GGA level, the two extra electrons are found to be fully delocalized on the lattice of Ti ions, and consequently, the solutions with singlet and triplet spin are degenerate. The corresponding energy levels lie at the bottom of the conduction band. The structural deformation of the lattice is very small and symmetric, with undercoordinated Ti ions around the vacancy showing only a slight relaxation with respect to their equilibrium positions. In contrast, with the hybrid B3LYP functional or the GGA+U method ($3\ \text{eV} \leq U \leq 4\ \text{eV}$), the ground state is a triplet; the two unpaired electrons prefer to localize on two different Ti ions, which are not necessarily undercoordinated.[28] For bulk anatase in particular, solutions have been obtained where (a) both electrons are localized at Ti sites, (b) one electron is localized and the other is delocalized, or (c) both electrons are delocalized (as in GGA).[28,29] At the B3LYP level, (a) and (b) are essentially degenerate, while solution (c) is 0.17 eV higher in energy.[28] These results show how delicate is the description of the unpaired electrons associated with the oxygen vacancy.

Ti Interstitial (Ti_{int})

For high-temperature annealing or prolonged thermal treatment there is evidence that Ti atoms or ions migrate from the surface layers into the bulk, where they occupy interstitial sites of the lattice. A Ti interstitial in principle introduces a total of four excess electrons, but the precise charge state of this defect is not obvious a priori. Calculations on bulk anatase[11,30−32] have shown that the Ti interstitial assumes a distorted pyramidal configuration and is coordinated to five oxygens. The corresponding electronic structure is characterized by several defect states in the band gap close to the bottom of the conduction band; these states are localized both on the Ti interstitial and on other hexacoordinate (Ti_{6c}) lattice sites in proximity to the defect. Calculations at the B3LYP level have shown that Ti_{int} traps only one electron, resulting in a formal charge +3 (Ti^{3+}),[30] whereas states corresponding to interstitial Ti^{2+} or Ti^+ ions are higher in energy. Thus, an important conclusion is that there is only one oxidation state possible for Ti interstitials.[30]

■ INTERACTION OF O_2 WITH THE REDUCED ANATASE (101) SURFACE

Anatase (101) is the most stable and frequent surface of the anatase phase.[2,33] It has the same periodicity as the bulk-truncated surface and exposes undercoordinated pentacoordinate Ti cations (Ti_{5c}) and dicoordinate oxygen anions (O_{2c}) as well as fully coordinated Ti_{6c} cations and tricoordinate O anions (O_{3c}) (Figure 1). The relaxed structure has been examined in detail in ref 33. It is characterized by outward ∼0.2 Å relaxations of the fully coordinated Ti_{6c} and O_{3c} surface atoms, while the Ti_{5c} atom relaxes inward, also by ∼0.2 Å, with respect to its position on the bulk-terminated surface.[33] As a result, the Ti_{5c}−O_{2c} bond on the relaxed surface (∼1.83 Å) is much shorter than that on the bulk-terminated one (∼2.00 Å). Besides contributing to the remarkable stability of anatase (101), the stiffness of the Ti_{5c}−O_{2c} bond can also explain why on anatase (101) oxygen vacancies are located not at the very surface but rather in subsurface layers or the bulk,[10−12] in contrast to what is observed on the rutile (110) surface.[2,4,16]

dx.doi.org/10.1021/ar400312t | Acc. Chem. Res. 2014, 47, 3361−3368

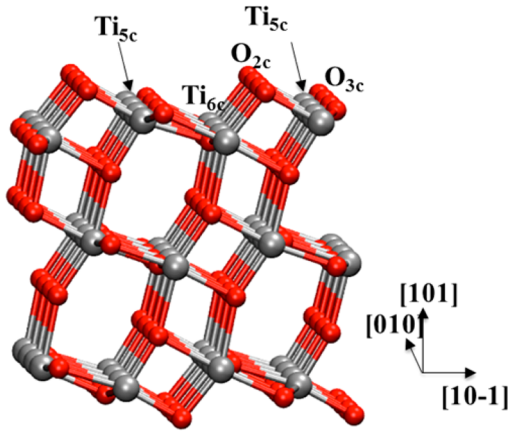

Figure 1. Side view of the anatase (101) surface showing the various types of exposed sites: undercoordinated (Ti_{5c}) and fully coordinated (Ti_{6c}) titanium atoms, bridging oxygens (O_{2c}), and fully coordinated oxygens (O_{3c}).

Reaction of O_2 with Subsurface Oxygen Vacancies

Figure 2a,c shows the density of states and excess electron density, respectively, of reduced anatase (101) with a subsurface oxygen vacancy computed using the DFT+U method (with U = 3.5 eV,[21] determined using linear response[34]). When a subsurface V_O is present, it is energetically favorable for O_2 to adsorb at a Ti_{5c} site close this defect.[21] The adsorption energy per O_2 molecule varies considerably with the separation between the defect and the O_2 molecule. An adsorption energy of 1.37 eV was computed for the Ti_{5c} site closest to the vacancy, whereas for a site at a distance of ~5.1 Å an adsorption energy of only 0.81 eV was found.[21] Upon adsorption, the extra charge associated with the defect (Figure 2a,c) is transferred to the O_2 molecule, converting it to a peroxide (O_2^{2-}) species. As shown by the density of states (Figure 2b), the transferred charge occupies the O_2 antibonding state, which lies in the anatase band gap. This is also reflected in the charge density distribution (Figure 2d), which shows a clear localization of the electron on the O_2 molecule with π^*-like character.

It was predicted theoretically that an O interstitial in bulk anatase would bind spontaneously with an O at a lattice site to form a substitutional O_2 molecule, $(O_2)_O$, which would have a bond length typical of a peroxide species.[31,35] A similar result was obtained for an O adatom at the (101) surface, where the adatom would bind with an O_{2c} atom to form a bridging dimer.[36] This $(O_2)_O$ species can be also regarded as the result of an O_2 molecule filling (i.e., "healing") a bulk or surface oxygen vacancy site. Interestingly, an analogous healing mechanism was found also for subsurface vacancies at the anatase (101) surface.[19] The reoxidation process was observed to occur spontaneously in first-principles molecular dynamics (FPMD)[37] simulations at $T \approx 220$ K with O_2 initially adsorbed at the site closest to the subsurface V_O defect,[19] and the pathway was further analyzed by nudged elastic band (NEB)[38] calculations. Selected snapshots along this pathway are shown in Figure 3, along with the corresponding potential energy profile (top panel). The latter shows an energy gain of about 1.6 eV from the state with O_2 adsorbed atop a subsurface V_O to the bridging dimer $(O_2)_O$ state, meaning that this transformation is energetically highly favorable. The process includes two main steps: diffusion of the oxygen vacancy from subsurface to the surface (from A to C) and filling of the

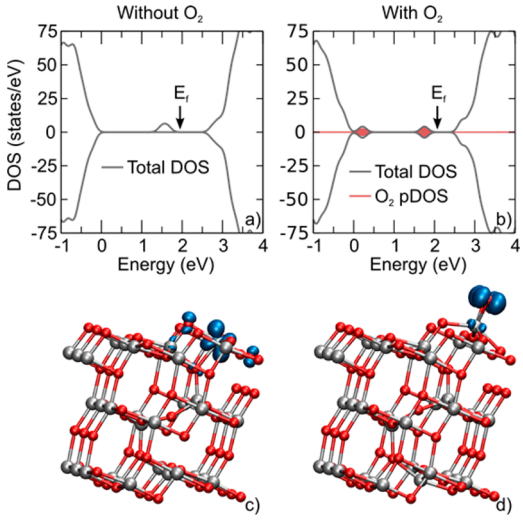

Figure 2. Electronic densities of states (upper panels) and HOMO charge densities (lower panels) for (a, c) a subsurface vacancy and (b, d) an O_2 molecule adsorbed in proximity to the subsurface vacancy. The energy zero is set at the valence-band maximum, and the Fermi energy (E_f) is indicated by arrows.

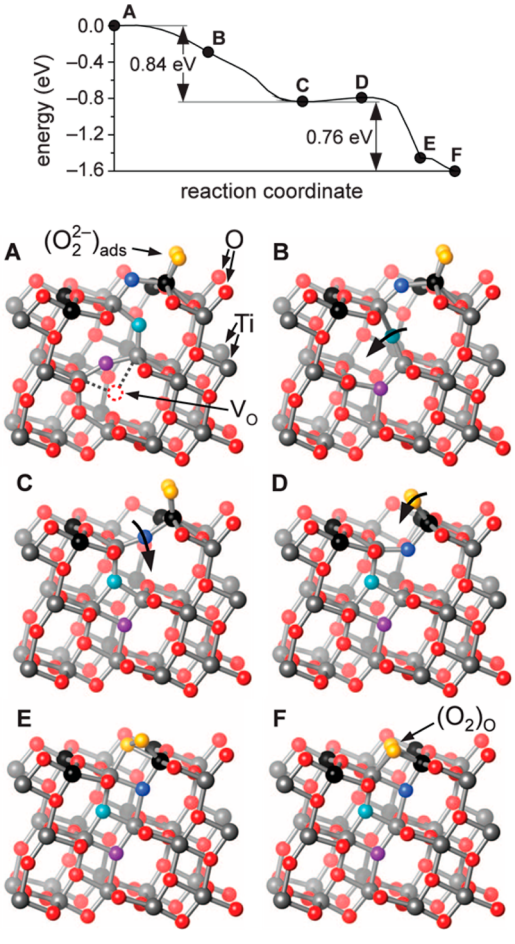

Figure 3. Potential energy profile and selected structure snapshots along the pathway leading from an adsorbed O_2 atop a subsurface oxygen vacancy to the bridging dimer state. (Adapted with permission from ref 19. Copyright 2013 American Association for the Advancement of Science.)

dx.doi.org/10.1021/ar400312t | Acc. Chem. Res. 2014, 47, 3361−3368

resulting surface vacancy by the adsorbed O_2. Both steps have very small barriers, the most significant one (between C and D in Figure 3) being associated with the approach of the molecule to the vacancy.

The process in Figure 3 was initially only a theoretical prediction but has been successively verified experimentally through extensive STM measurements.[19] Besides being by far the most stable O_2 species on the anatase surface, the bridging dimer has been proposed to be an important intermediate in the oxygen evolution reaction on anatase (101)[36] and may also contribute to the higher catalytic activity of anatase with respect to rutile.[6]

Reaction of O_2 with Ti Interstitials

As mentioned earlier, a Ti_{int} defect introduces a total of four excess electrons. One of these remains localized in the 3d shell of the Ti interstitial to form a Ti^{3+} species with energy about 1 eV below the bottom of the conduction band, whereas the other three electrons are donated to lattice Ti ions close to Ti_{int} to form states with mixed localized/delocalized character at or near the bottom of the conduction band.[30] The location of Ti_{int} and the associated excess electrons has a marked effect on the adsorption energetics of O_2 atop Ti interstitials.[39] The computed O_2 adsorption energy can be as large as 2.5 eV when Ti_{int} is in the first subsurface TiO_2 layer, whereas it does not exceed 1.9 eV when Ti_{int} is located in the second layer below the surface, indicating less favorable charge transfer to the adsorbed molecule. This effect is also reflected in variations of the adsorption energy for different sites atop the same interstitial. For an interstitial in the first subsurface layer, the O_2 adsorption energy shows variations as large as 1.1 eV, with stronger binding at Ti sites closer to Ti_{int}. These variations are much smaller (0.45 eV) when the interstitial is in the second subsurface layer.[39]

Similarly to what was found for subsurface V_O's, the state with O_2 adsorbed atop a subsurface Ti interstitial is only metastable. There is in fact a state with much lower energy, where, after migration to the surface, Ti_{int} recombines with O_2 to form an adsorbed TiO_2 cluster. The computed minimum-energy pathway for this process is shown in Figure 4. While it is energetically favorable for Ti_{int} to reside in the subsurface in the absence of adsorbed O_2, migration to the surface becomes exothermic when an adsorbed O_2 is present (step 5 in Figure 4). The migration barrier is also slightly reduced, from 0.88 eV without O_2 to 0.84 eV in the presence of adsorbed O_2 [gray and black lines, respectively, in the left-side (phase 1) part of Figure 4]. Once at the surface, T_{int} can split the O_2 molecule and form a small TiO_2 island with a very large energy gain of 3.57 eV (step 7 in Figure 4). A further rearrangement with a barrier of 1.57 eV can convert this structure into the final state (step 9 in Figure 4), which is over 4.5 eV lower in energy than the initial state with the O_2 molecule adsorbed atop the subsurface interstitial.

The direct diffusion mechanism described above is not the only possible pathway for the Ti interstitial to migrate to the surface. NEB calculations identified an additional "exchange" pathway in which the interstitial replaces the Ti atom to which the O_2 is bound (dashed line in Figure 4). An analogous pathway was predicted to occur on rutile (110).[14] For the exchange pathway in Figure 4, an initial barrier of 0.47 eV is associated with the breaking of the O−O bond and the transformation to a structure similar to that of step 5 in the direct pathway. After a large energy drop accompanying a

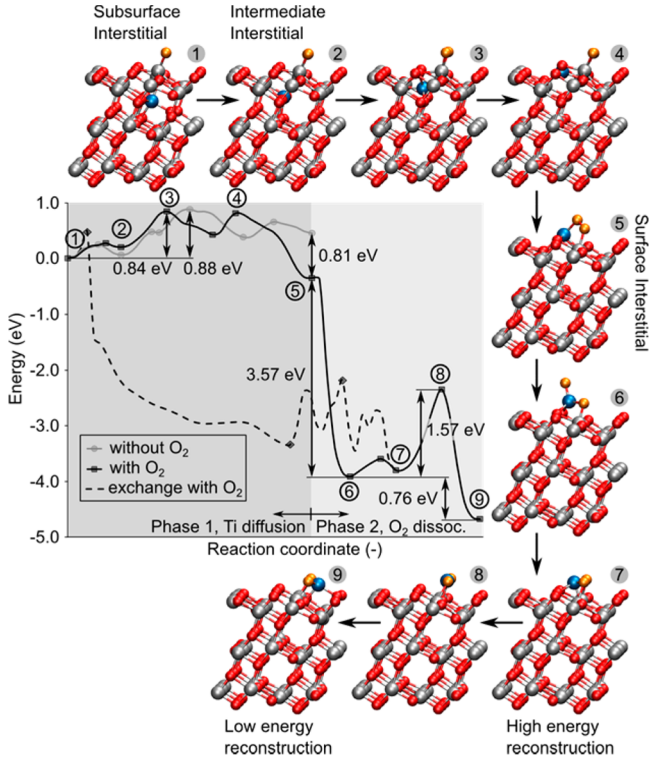

Figure 4. Potential energy profile and selected structures along the pathway leading from an adsorbed O_2 atop a Ti interstitial to an adsorbed TiO_2 species. Solid line, direct pathway; dashed line, exchange pathway. The structures shown refer to the direct pathway.

conversion similar to the one from step 5 to step 6, there are two energy barriers of approximately 1 eV associated with the two-step diffusion of the interstitial to the surface, whereas the last barrier is associated with the rearrangement of the O_2 fragments, similar to the transition from step 6 to step 7 in the direct pathway. To some extent, the sequence of events for the direct and exchange pathways are inverted: for the former the breaking of the bond in the O_2 molecule occurs after the diffusion of the interstitial to the surface, whereas for the latter the breaking of the O_2 bond occurs first.

An important conclusion from the above studies is that O_2 promotes the migration of reducing subsurface defects (Ti interstitials and oxygen vacancies) to the surface. In other words, the distribution and dynamics of the defects in the material depend on the surrounding environment. This effect has been observed in other oxides as well; in particular, it is the basis of the activity of SnO_2 as a gas sensor.[40] For subsurface oxygen vacancies the interaction with O_2 leads to oxygen incorporation, whereas for Ti interstitials it leads to the growth of TiO_2 islands. The latter process is also responsible for the strong metal−support interaction (SMSI) effect,[41,42] which plays an important role in heterogeneous catalysis. The oxygen-induced migration of Ti interstials has been observed experimentally on the rutile (110) surface.[14,43]

CHARGE STATES OF ADSORBED O_2

We have already pointed out that DFT calculations consistently predict a considerably greater stability of the peroxide state relative to other charge states,[44] thus preventing a detailed interpretation of the EPR observation of adsorbed superoxide species.[8,18] This difficulty has motivated recent hybrid functional investigations[45] of the (I) one- and (II) two-electron-

dx.doi.org/10.1021/ar400312t | Acc. Chem. Res. 2014, 47, 3361−3368

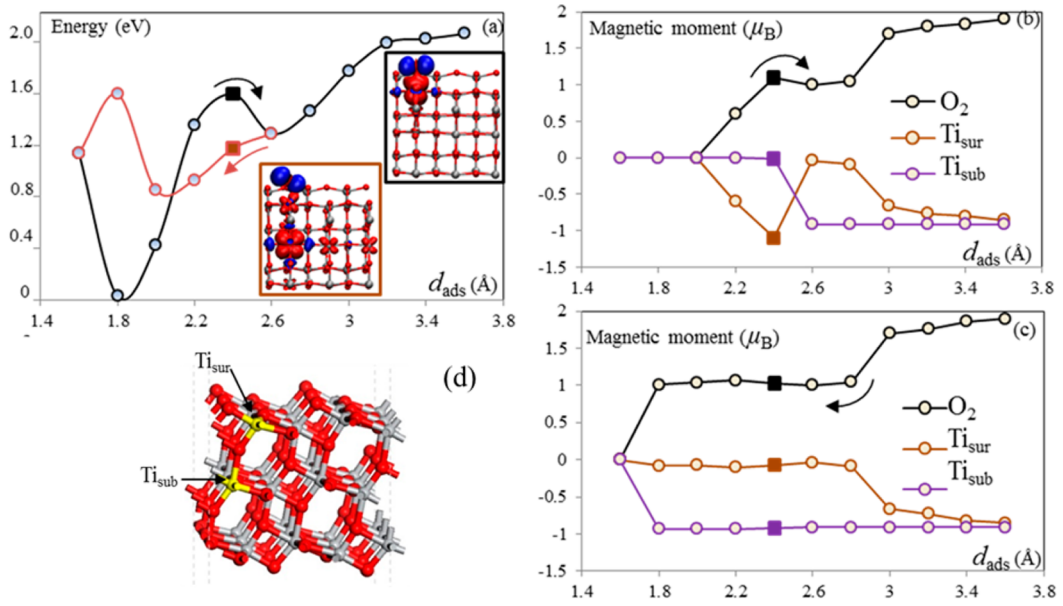

Figure 5. (a) Energy profile and (b, c) magnetic moments for reaction II. The arrow indicates the scan direction along the reaction coordinate (d_{ads}). The insets in (a) show the spin densities at d_{ads} = 2.4 Å along the inward (red box on the left) and outward (black box on the right) scan directions. The isosurface for the spin density is 0.001 au with blue = positive and red = negative. Computed values are shown as circles (or as solid squares at d_{ads} = 2.4 Å). (d) Anatase (101) slab model used for the calculations. Oxygens are red, Ti atoms are gray. The two yellow spheres indicate Ti_{sur} and Ti_{sub}, the localization sites of the extra electrons added to describe the reduced surface. (Reprinted from ref 45. Copyright 2013 American Chemical Society).

transfer reactions between reduced anatase (101) and molecular O_2:

$$* + O_2(g) \rightleftarrows *O_2^- \quad \text{(I)}$$

$$* + O_2(g) \rightleftarrows *O_2^{2-} \quad \text{(II)}$$

where $*$ denotes a Ti_{5c} adsorption site of the reduced anatase (101) surface, $O_2(g)$ represents a gas-phase oxygen molecule, and $*O_2^-$ ($*O_2^{2-}$) denotes an adsorbed superoxide (peroxide) species. The reduced surface was modeled by adding two excess electrons per supercell to the slab and introducing a compensating uniform background charge to make the overall system charge-neutral; test calculations to validate the results obtained with this model are discussed in the following. After structural optimization, the two excess electrons localized spontaneously at a surface Ti_{5c} atom (Ti_{sur}) and a subsurface Ti_{6c} site (Ti_{sub}) (see Figure 5d). Configurations with both electrons at surface sites were also considered, but these were found to be at least 0.14 eV higher in energy (the difference was even larger, 0.27 eV, for the reduced neutral slab model described in the following). The potential energy surfaces of reactions I and II were scanned using the distance between the center of mass of the O_2 molecule and Ti_{sur} (d_{ads}) as the reaction coordinate. For each reaction, two energy profiles were calculated by varying the reaction coordinate both outward (i.e., from small to large d_{ads}) and inward (i.e., from large to small d_{ads}).

For reaction I, the electron transfer (ET) process turns out to be *barrierless*, and neither the potential energy surface nor the magnetic moments of O_2 and Ti_{sur} along the reaction coordinate depend on the scan direction of the reaction coordinate. For reaction II, however, the energy profiles for the inward and outward scans are different (Figure 5a). Analysis of the magnetic moments (Figure 5b,c) clearly shows that the reaction occurs in two steps, corresponding to successive transfers of the two electrons. In the outward pathway, O_2^{2-} loses an electron to the surface at $d_{ads} \approx 2.4$ Å, while the resulting superoxide O_2^- transfers its excess electron to the surface at $d_{ads} \approx 3$ Å. In the inward pathway, transfer of the first electron from Ti_{sur} to O_2 to form O_2^- occurs at $d_{ads} \approx 3$ Å, while the transfer of the second electron from Ti_{sub} to O_2^- to form O_2^{2-} occurs at much shorter distance, $d_{ads} \approx 1.8$ Å. Significant differences between the inward and outward pathways are also present for the spin densities, as shown at d_{ads} = 2.4 Å in the Figure 5a insets.

The hysteresis in the potential energy profile for reaction II was explained on the basis of the Marcus theory of electron transfer[46,47] in ref 45. According to this theory, the ET rate is determined by two factors, the diabatic barrier and the electronic coupling between the two electronic states. When the coupling is strong, the ET is "adiabatic". In this case, the calculated energy profiles always follow the adiabatic potential surface, and no hysteresis can occur, as found for reaction I. If the coupling is weak, the ET is "nonadiabatic". In this case, the calculated energy profile may follow one diabatic potential surface and suddenly jump to another diabatic potential surface, and an energy profile of the type shown in Figure 5a can then be observed.

The results in Figure 5 also suggest the existence of an energy barrier for ET between the superoxide and peroxide species. This barrier was estimated by a simple approach[48] that consisted of performing total energy calculations on a series of linearly interpolated geometries between the optimized geometries of the $*O_2^-$ and $*O_2^{2-}$ species. In this way, a significant barrier of ~0.3 eV between the superoxo and peroxo states was obtained (Figure 6).

Altogether, the results presented in this section seem to provide a satisfactory explanation of the differences between the DFT calculations and experimental results for O_2 adsorption on anatase TiO_2. However, there is still a technical point that

dx.doi.org/10.1021/ar400312t | Acc. Chem. Res. 2014, 47, 3361−3368

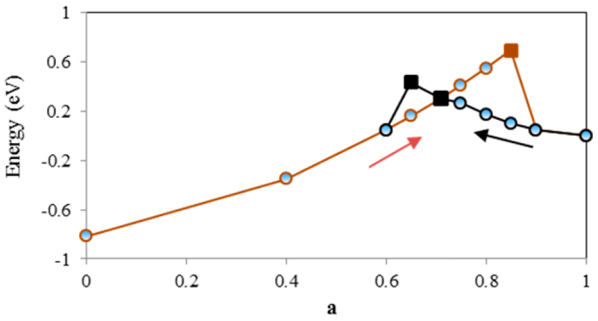

Figure 6. Energy profile for electron transfer between the superoxo $*O_2^-$ (**a** = 1) and peroxo $*O_2^{2-}$ (**a** = 0) states, where **a** is the reaction coordinate. The arrows indicate the scan direction along **a**. Computed values are shown as circles [or as solid squares at the transition state (**a** = 0.71) and the break points (**a** = 0.65 and 0.85)]; lines are a guide for the eye. (Reprinted from ref 45. Copyright 2013 American Chemical Society).

needs to be clarified before this explanation can be fully accepted. Since periodic charged slab models with a compensating background (of the type used for the studies described above) can lead to an unphysical dependence of the results on the width of the vacuum region between adjacent slabs,[49,50] it is important to verify that the results in Figures 5 and 6 remain substantially unchanged when the model used for the calculations is changed. To address this question, the reduced surface was modeled as a *neutral* slab with two adsorbed H atoms on the bottom surface. Figure 7 shows a comparison between the potential energy profiles for reaction II (outward scans) with and without the compensating background. The two profiles are very similar at small distances ($d_{ads} \leq 2.4$ Å), but there is clearly a difference at large distances ($d_{ads} > 2.4$ Å), confirming that periodic charged slab models should

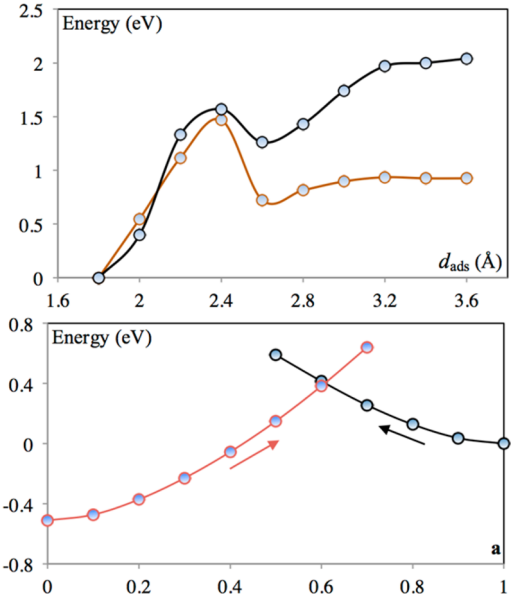

Figure 7. (top) Potential energy profiles for reaction II scanned along the outward direction of the reaction coordinate d_{ads}. Black and red dots refer to calculations using a charged slab with compensating background charge and a neutral slab, respectively. (bottom) Energy profile for electron transfer between the adsorbed superoxo $*O_2^-$ (**a** = 1) and peroxo $*O_2^{2-}$ (**a** = 0) states for a neutral slab, where **a** is the reaction coordinate. The arrows indicate the scan direction along **a**.

indeed be used with much care. At the same time, however, it appears that at d_{ads} >2.4 Å the electron transfer from $*O_2^{2-}$ to the surface to form $*O_2^-$ is already complete, suggesting that the energy barrier between the peroxo and superoxo states may not be significantly affected. In fact, a calculation of this barrier using the neutral slab with reducing H adatoms gave a value of ~0.4 eV (Figure 7), which is well-consistent with the ~0.3 eV barrier in Figure 6.

CONCLUDING REMARKS

In this Account, we have discussed two important aspects of the interaction of O_2 with the reduced anatase TiO_2 surface: the charge states of adsorbed O_2 and the interaction of O_2 with subsurface oxygen vacancies and titanium interstitials.

The existence of a kinetic barrier between the superoxo and peroxo states is essential for understanding a series of experimental results. First of all, it allows us to explain why superoxo species are generally observed experimentally.[8,18] Although the peroxo $*O_2^{2-}$ species is energetically more stable than $*O_2^-$, there is a significant barrier of ~0.3−0.4 eV that must be overcome to transfer an additional electron to $*O_2^-$ (whose formation is barrierless) and transform it to a peroxide. Additionally, kinetic studies have provided evidence that O_2 is not very efficient as an electron scavenger and may limit the overall photocatalytic rate.[51−56] By analyzing various mechanistic models, Gerischer and Heller[56] showed that the overall quantum efficiency of large TiO_2 particles ($R > 1$ μm) is limited not by the diffusion of O_2 but rather by the rate of ET to adsorbed O_2. Successively, Wang et al.[53] provided experimental evidence that electrons accumulate on TiO_2 particles during the photocatalytic oxidation of aqueous methanol. The existence of a kinetic barrier of ~0.3−0.4 eV between superoxo and peroxo states provides a fundamental explanation for the observed limited efficiency of O_2 as an electron scavenger.

As for the interaction mechanisms of O_2 with oxygen vacancies and titanium interstitials on anatase (101), the results discussed here show that defects are not just a static source of negative charge to enable the formation of adsorbed superoxo or peroxo species. Instead, they actively take part in the reaction with O_2 even though they are located in subsurface layers. Adsorption of molecular oxygen favors the migration of the defects toward the surface. Titanium interstitials can then exothermically react to form TiO_2-like islands on the surface, whereas oxygen vacancies can accommodate O_2 molecules in the bridging dimer configuration. Hence, both types of reducing intrinsic defects provide energetically favorable pathways for the incorporation of O_2 into anatase TiO_2.

AUTHOR INFORMATION

Corresponding Author

*E-mail: aselloni@princeton.edu.

Notes

The authors declare no competing financial interest.

Biographies

Ye-Fei Li is a postdoctoral fellow in the Department of Chemistry at Princeton University. He received his Ph.D. degree from Fudan University (Shanghai, China) in 2012. His main research interest is in catalysis on oxide surfaces.

Ulrich Aschauer is a postdoctoral fellow in the Materials Theory Group at ETH Zürich after a previous postdoctoral position at Princeton. He received his Ph.D. degree from EPFL (Lausanne,

Switzerland) in 2008. His main research interest is in the physicochemical properties of oxide materials.

Jia Chen is a postdoctoral fellow in the Physics Department at Columbia University. He received his Ph.D. degree from Princeton University in 2013. His main research interest is in the electronic structure of complex oxides.

Annabella Selloni is the David B. Jones Professor of Chemistry at Princeton University. Prior to joining the faculty at Princeton in 2002, she held positions at the University "La Sapienza" (Roma, Italy), the International School for Advanced Studies (Trieste, Italy), and the University of Geneva (Switzerland). She has coauthored ∼250 publications, mostly in the fields of surface physics and chemistry. Her current research interests are mainly focused on metal oxide materials, surfaces, and interfaces; photocatalysis; and photovoltaics.

■ ACKNOWLEDGMENTS

We thank Ulrike Diebold for many helpful discussions. This work was supported by DOE-BES, Division of Chemical Sciences, Geosciences, and Biosciences, under Award DE-FG02-12ER16286. We used resources of the National Energy Research Scientific Computing Center (DOE Contract DE-AC02-05CH11231). We also acknowledge use of the TIGRESS high-performance computer center at Princeton University.

■ REFERENCES

(1) Linsebigler, A. L.; Lu, G.; Yates, J. T., Jr. Photocatalysis on TiO_2. *Chem. Rev.* **1995**, *95*, 735−758.
(2) Diebold, U. The surface science of titanium dioxide. *Surf. Sci. Rep.* **2003**, *48*, 53−229.
(3) Fujishima, A.; Zhang, X.; Tryk, D. A. TiO_2 photocatalysis and related surface phenomena. *Surf. Sci. Rep.* **2008**, *63*, 515−582.
(4) Henderson, M. A. A surface science perspective on TiO_2 photocatalysis. *Surf. Sci. Rep.* **2011**, *66*, 185−297.
(5) Zhang, H. Z.; Banfield, J. F. Thermodynamic analysis of phase stability of nanocrystalline titania. *J. Mater. Chem.* **1998**, *8*, 2073−2076.
(6) Kavan, L.; Grätzel, M.; Gilbert, S. E.; Klemenz, C.; Scheel, H. J. Electrochemical and Photoelectrochemical Investigation of Single-Crystal Anatase. *J. Am. Chem. Soc.* **1996**, *118*, 6716−6723.
(7) Grätzel, M. Photoelectrochemical Cells. *Nature* **2001**, *414*, 338−344.
(8) Berger, T.; Sterrer, M.; Diwald, O.; Knözinger, E.; Panayotov, D.; Thompson, T. L.; Yates, J. T., Jr. Light-Induced Charge Separation in Anatase TiO_2 Particles. *J. Phys. Chem. B* **2005**, *109*, 6061−6068.
(9) Di Valentin, C.; Pacchioni, G.; Selloni, A. Reduced and n-Type Doped TiO_2: Nature of Ti^{3+} Species. *J. Phys. Chem. C* **2009**, *113*, 20543−20552.
(10) Cheng, H.; Selloni, A. Surface and subsurface oxygen vacancies in anatase TiO_2 and differences with rutile. *Phys. Rev. B* **2009**, *79*, No. 092101.
(11) Cheng, H.; Selloni, A. Energetics and diffusion of intrinsic surface and subsurface defects on anatase $TiO_2(101)$. *J. Chem. Phys.* **2009**, *131*, No. 054703.
(12) He, Y.; Dulub, O.; Cheng, H.; Selloni, A.; Diebold, U. Evidence for the Predominance of Subsurface Defects on Reduced Anatase $TiO_2(101)$. *Phys. Rev. Lett.* **2009**, *102*, No. 106105.
(13) Wendt, S.; Schaub, R.; Matthiesen, J.; Vestergaard, E. K.; Wahlström, E.; Rasmussen, M. D.; Thostrup, P.; Molina, L. M.; Lægsgaard, E.; Stensgaard, I.; Hammer, B.; Besenbacher, F. Oxygen vacancies on $TiO_2(110)$ and their interaction with H_2O and O_2: A combined high-resolution STM and DFT study. *Surf. Sci.* **2005**, *598*, 226−245.
(14) Wendt, S.; Sprunger, P. T.; Lira, E.; Madsen, G. K. H.; Li, Z.; Hansen, J. Ø.; Matthiesen, J.; Blekinge-Rasmussen, A.; Lægsgaard, E.; Hammer, B.; Besenbacher, F. The role of interstitial sites in the Ti 3d defect state in the band gap of titania. *Science* **2008**, *320*, 1755−1759.
(15) Petrik, N. G.; Zhang, Z. R.; Du, Y. G.; Dohnálek, Z.; Lyubinetsky, I.; Kimmel, G. A. Chemical Reactivity of Reduced $TiO_2(110)$: The Dominant Role of Surface Defects in Oxygen Chemisorption. *J. Phys. Chem. C* **2009**, *113*, 12407−12411.
(16) Dohnálek, Z.; Lyubinetsky, I.; Rousseau, R. Thermally-driven processes on rutile $TiO_2(110)$-(1×1): A direct view at the atomic scale. *Prog. Surf. Sci.* **2010**, *85*, 161−205.
(17) Scheiber, P.; Riss, A.; Schmid, M.; Varga, P.; Diebold, U. Observation and Destruction of an Elusive Adsorbate with STM: O_2/$TiO_2(110)$. *Phys. Rev. Lett.* **2010**, *105*, No. 216101.
(18) Carter, E.; Carley, A. F.; Murphy, D. M. Evidence for O_2^- radical stabilization at surface oxygen vacancies on polycrystalline TiO_2. *J. Phys. Chem. C* **2007**, *111*, 10630−10638.
(19) Setvin, M.; Aschauer, U.; Scheiber, P.; Li, Y. F.; Hou, W.; Schmid, M.; Selloni, A.; Diebold, U. Reaction of O_2 with subsurface oxygen vacancies on TiO_2 anatase (101). *Science* **2013**, *341*, 988−991.
(20) Mattioli, G.; Filippone, F.; Bonapasta, A. A. Reaction Intermediates in the Photoreduction of Oxygen Molecules at the (101) TiO_2 (Anatase) Surface. *J. Am. Chem. Soc.* **2006**, *128*, 13772−13780.
(21) Aschauer, U.; Chen, J.; Selloni, A. Peroxide and superoxide states of adsorbed O_2 on anatase $TiO_2(101)$ with subsurface defects. *Phys. Chem. Chem. Phys.* **2010**, *12*, 12956−12960.
(22) Perdew, J. P.; Burke, K.; Ernzerhof, M. Generalized Gradient Approximation Made Simple. *Phys. Rev. Lett.* **1996**, *77*, 3865−3868.
(23) Ganduglia-Pirovano, V. M.; Hofmann, A.; Sauer, J. Oxygen vacancies in transition metal and rare earth oxides: Current state of understanding and remaining challenges. *Surf. Sci. Rep.* **2007**, *62*, 219−270.
(24) Cohen, A. J.; Mori-Sanchez, P.; Yang, W. T. Insights into current limitations of density functional theory. *Science* **2008**, *321*, 792−794.
(25) Anisimov, V. I.; Zaanen, J.; Andersen, O. K. Band theory and Mott insulators: Hubbard *U* instead of Stoner *I*. *Phys. Rev. B* **1991**, *44*, 943−954.
(26) Becke, A. D. Density-functional thermochemistry. III. The role of exact exchange. *J. Chem. Phys.* **1993**, *98*, 5648−5652.
(27) Perdew, J. P.; Ernzerhof, M.; Burke, K. Rationale for mixing exact exchange with density functional approximations. *J. Chem. Phys.* **1996**, *105*, 9982−9985.
(28) Finazzi, E.; Di Valentin, C.; Pacchioni, G.; Selloni, A. Excess electron states in reduced bulk anatase TiO_2: Comparison of standard GGA, GGA+U, and hybrid DFT calculations. *J. Chem. Phys.* **2008**, *129*, No. 154113.
(29) Mattioli, G.; Filippone, F.; Alippi, P.; Bonapasta, A. A. Ab initio study of the electronic states induced by oxygen vacancies in rutile and anatase TiO_2. *Phys. Rev. B* **2008**, *78*, No. 241201.
(30) Finazzi, E.; Di Valentin, C.; Pacchioni, G. Nature of Ti Interstitials in Reduced Bulk Anatase and Rutile TiO_2. *J. Phys. Chem. C* **2009**, *113*, 3382−3385.
(31) Na-Phattalung, S.; Smith, M. F.; Kwiseon, K.; Mao-Hua, D.; Su-Huai, W.; Zhang, S. B.; Sukit, L. First-principles study of native defects in anatase TiO_2. *Phys. Rev. B* **2006**, *73*, No. 125205.
(32) Mattioli, G.; Alippi, P.; Filippone, F.; Caminiti, R.; Bonapasta, A. A. Deep versus Shallow Behavior of Intrinsic Defects in Rutile and Anatase TiO_2 Polymorphs. *J. Phys. Chem. C* **2010**, *114*, 21694−21704.
(33) Lazzeri, M.; Vittadini, A.; Selloni, A. Structure and energetics of stoichiometric TiO_2 anatase surfaces. *Phys. Rev. B* **2001**, *63*, No. 155409.
(34) Cococcioni, M.; de Gironcoli, S. Linear response approach to the calculation of the effective interaction parameters in the LDA+U method. *Phys. Rev. B* **2005**, *71*, No. 035105.
(35) Kamisaka, H.; Yamashita, K. Theoretical Study of the Interstitial Oxygen Atom in Anatase and Rutile TiO_2: Electron Trapping and Elongation of the r(O−O) Bond. *J. Phys. Chem. C* **2011**, *115*, 8265−8273.
(36) Li, Y.-F.; Liu, Z.-P.; Liu, L.; Gao, W. Mechanism and Activity of Photocatalytic Oxygen Evolution on Titania Anatase in Aqueous Surroundings. *J. Am. Chem. Soc.* **2010**, *132*, 13008−13015.

(37) Car, R.; Parrinello, M. Unified approach for molecular dynamics and density-functional theory. *Phys. Rev. Lett.* **1985**, *55*, 2471−2474.
(38) Henkelman, G.; Uberuaga, B. P.; Jónsson, H. A climbing image nudged elastic band method for finding saddle points and minimum energy paths. *J. Chem. Phys.* **2000**, *113*, 9901−9904.
(39) Aschauer, U.; Selloni, A. Influence of subsurface Ti interstitials on the reactivity of anatase (101). *Proc. SPIE* **2010**, *7758*, No. 77580B.
(40) Lopez, N.; Prades, J. D.; Hernandez-Ramirez, F.; Morante, J. R.; Pan, J.; Mathur, S. Bidimensional versus tridimensional oxygen vacancy diffusion in SnO_{2-x} under different gas environments. *Phys. Chem. Chem. Phys.* **2010**, *12*, 2401−2406.
(41) Dulub, O.; Hebenstreit, W.; Diebold, U. Imaging cluster surfaces with atomic resolution. The strong metal−support interaction state of Pt supported on TiO_2(110). *Phys. Rev. Lett.* **2000**, *84*, 3646−3649.
(42) Fu, Q.; Wagner, T. Interaction of nanostructured metal overlayers with oxide surfaces. *Surf. Sci. Rep.* **2007**, *62*, 431−498.
(43) Zhang, Z.; Lee, J.; Yates, J. T., Jr.; Bechstein, R.; Lira, E.; Hansen, J. Ø.; Wendt, S.; Besenbacher, F. Unraveling the Diffusion of Bulk Ti Interstitials in Rutile TiO_2(110) by Monitoring Their Reaction with O Adatoms. *J. Phys. Chem. C* **2010**, *114*, 3059−3062.
(44) Filippone, F.; Mattioli, G.; Bonapasta, A. A. Reaction intermediates and pathways in the photoreduction of oxygen molecules at the (101) TiO_2 (anatase) surface. *Catal. Today* **2007**, *129*, 169−176.
(45) Li, Y.-F.; Selloni, A. Theoretical Study of Interfacial Electron Transfer from Reduced Anatase TiO_2(101) to Adsorbed O_2. *J. Am. Chem. Soc.* **2013**, *135*, 9195−9199.
(46) Marcus, R. A. On the Theory of Oxidation−Reduction Reactions Involving Electron Transfer. I. *J. Chem. Phys.* **1956**, *24*, 966−978.
(47) Marcus, R. A. Electrostatic Free Energy and Other Properties of States Having Nonequilibrium Polarization. I. *J. Chem. Phys.* **1956**, *24*, 979−989.
(48) Deskins, N. A.; Dupuis, M. Electron transport via polaron hopping in bulk TiO_2: A density functional theory characterization. *Phys. Rev. B* **2007**, *75*, No. 195212.
(49) Komsa, H.-P.; Pasquarello, A. Finite-Size Supercell Correction for Charged Defects at Surfaces and Interfaces. *Phys. Rev. Lett.* **2013**, *110*, No. 095505.
(50) Richter, N. A.; Sicolo, S.; Levchenko, S. V.; Sauer, J.; Scheffler, M. Concentration of Vacancies at Metal-Oxide Surfaces: Case Study of MgO(100). *Phys. Rev. Lett.* **2013**, *111*, No. 045502.
(51) Gerischer, H. Electron-transfer kinetics of redox reactions at the semiconductor/electrolyte contact. A new approach. *J. Phys. Chem.* **1991**, *95*, 1356−1359.
(52) Gerischer, H. Photoelectrochemical catalysis of the oxidation of organic molecules by oxygen on small semiconductor particles with TiO_2 as an example. *Electrochim. Acta* **1993**, *38*, 3−9.
(53) Wang, C. M.; Heller, A.; Gerischer, H. Palladium catalysis of O_2 reduction by electrons accumulated on TiO_2 particles during photoassisted oxidation of organic compounds. *J. Am. Chem. Soc.* **1992**, *114*, 5230−5234.
(54) Peiró, A. M.; Colombo, C.; Doyle, G.; Nelson, J.; Mills, A.; Durrant, J. R. Photochemical Reduction of Oxygen Adsorbed to Nanocrystalline TiO_2 Films: A Transient Absorption and Oxygen Scavenging Study of Different TiO_2 Preparations. *J. Phys. Chem. B* **2006**, *110*, 23255−23263.
(55) Gerischer, H.; Heller, A. The role of oxygen in photooxidation of organic molecules on semiconductor particles. *J. Phys. Chem.* **1991**, *95*, 5261−5267.
(56) Gerischer, H.; Heller, A. Photocatalytic Oxidation of Organic Molecules at TiO_2 Particles by Sunlight in Aerated Water. *J. Electrochem. Soc.* **1992**, *139*, 113−118.